Materials and methods

Cell lines and cell culture

Human OC cell lines (HO8910, HO8910-PM and A2780) were provided by Women's Hospital, Zhejiang University School of Medicine, where they were tested and authenticated as described previously(Shen et al., 2021; Shen et al., 2022). All cells were cultured in RPMI 1640 (BI, Israel) medium containing 10% fetal bovine serum (FBS) in a 5% CO_2 humidified incubator at 37℃.

RNA sequencing analysis

Total RNA was extracted from HO8910 cells (n = 1) and HO8910PM cells (n = 1) using TRIzol Reagent (Invitrogen, USA). RNA quality was evaluated using an Agilent 2200 instrument (Agilent, USA). High-quality RNA was used for sequencing. First, the rRNA was removed and fragmented to obtain fragments approximately 200 nucleotides in length. Complementary DNA (cDNA) was then synthesized and purified. Third, the ends of the cDNA were repaired and primers were added for PCR amplification and purification. Finally, after quality inspection, libraries were sequenced using the Illumina HiSeq Platform (RiboBio Co., Ltd., China).

Patients and tissue samples

Forty-nine samples of OC patients and eight samples of patients with nonmalignant ovarian tissue who underwent surgery for the first time, without any radiotherapy, chemotherapy, or neoadjuvant chemotherapy before surgery were obtained. The patient information is provided in Table S1. Patients with other malignant tumors or severe complicated diseases were excluded. Informed consent was obtained from all participants. These excised tissue samples from patients were immediately snap-frozen in liquid nitrogen and then stored at − 80 °C until use. Tissue samples were used for detecting expression of candidate lncRNA RAD51B-AS1 and candidate gene RAD51B by RT-qPCR.

RNA extraction and RT-qPCR

Total RNA from tissues and cells was extracted using TRIzol Reagent. Nuclear and cytoplasmic fractions were isolated using the PARIS Kit RNA Isolation System (Invitrogen, Thermo Fisher Scientific). The PrimeScript RT reagent Kit with gDNA Eraser (Takara Bio Inc.) was used to synthesize cDNA, and RT-qPCR was performed using TB Green Premix Ex Taq (Takara Bio Inc.). Primers' sequences are provided in Table S2. Statistical analyses were performed using the $2^{-\Delta\Delta C_T}$ relative quantification method.

Northern blotting

Probes were prepared and digoxigenin-labeled by Sangon Biotech Co., Ltd. (Shanghai, China), and their sequences are listed in Table S3. Next, 15 μg of RNA was separated in a 1% formaldehyde denatured gel after electrophoresis under a constant voltage of 25 V and low temperature overnight and subsequently transferred to a HyBond N+ membrane by the upward capillary transfer method for 20 h. The membrane was pre-hybridized in a hybrid furnace at 50°C for 2 h and hybridized overnight in a 50°C hybridization apparatus. Then, the film was blocked for 1 h and reacted with the antibody solution for 30 min. The final step was X-ray film exposure and recording of the results in the darkroom.

Transfection of siRNA and lentiviral vectors into OC cells

siRNAs purchased from GenePharm (Shanghai, China) were used to knock down *RAD51B-AS1* or *RAD51B*, and their efficiency was evaluated by RT-qPCR. These sequences are

listed in Table S4. Additionally, for the ectopic expression of RAD51B-AS1, lentiviruses encoding the *RAD51-AS1* sequence and negative control lentiviruses (LV-*RAD51B-AS1* and LV-NC, respectively; GeneChem, Shanghai, China) were used to infect HO8910 cells. After 72 h of infection, the cells were selected using a complete culture medium containing 2 μg/mL puromycin.

Cell Counting Kit-8 assay

Cell proliferation was assessed using the Cell Counting Kit-8 (CCK-8) assay (Dojindo Laboratories, Japan). Cells were seeded at a density of 5 × 103 cells/well into 96-well plates. CCK-8 solution (10 μL) was added to each well at hours 0h, 24h, 48h, 72h and 96h post-transfection. After incubation at 37°C for 2 h, the absorbance at 450 nm was measured by a microplate reader (SkanIt RE for Varioskan Flash 2.4.3).

Plate colony-formation assay and soft-agar colony-formation assay

For plate colony-formation assays, 500 cells per well were resuspended, added to six-well plates, and incubated at 37 °C for 2 weeks. For soft-agar colony-formation assays, 5000 cells per well were resuspended in complete culture medium containing 0.3% agarose, added to six-well plates already solidified by medium containing 0.5% agarose, and incubated for 3 weeks as previously described(Ye et al., 2020). The colonies were fixed and stained with 0.1% crystal violet for 20 min. Cell colonies (>50 cells) were counted and analyzed per well.

Transwell migration and invasion assay

Cell migration and invasion assays were conducted using 24-well Transwell plates (8 μm pores; Corning Costar, USA). Transwell filter inserts were coated with (invasion) or without (migration) Matrigel (BD Biosciences, 1:12 dilution). A total of 3×10^5 cells (invasion) or 2×10^5 cells (migration) suspended in 200 μL of OPTI-MEM were added to the upper chamber, and 500 μL of high-concentration medium containing 18% FBS was added to the lower chamber, while avoiding air bubbles between the upper and lower chambers. After incubation for 24 h, the cells that traversed the bottom of the upper chamber were fixed in 0.5% crystal violet solution for 20 min. The cells remaining in the upper chamber were removed using cotton swabs. Images were captured and the number of cells per field was counted.

Establishment of anoikis model

Adherent OC cells were digested with 0.25% trypsin and added to a six-well plate with an ultra-low attachment surface (polystyrene, non-pyrogenic) purchased from Corning, with approximately 2.5×10^5 cells per well. Under these conditions, the morphology and growth of suspended cells were observed by microscopy. The culture medium was changed once every 2 or 3 days depending on the state of the cells (medium changing method: after centrifugation at 800 rpm for 3 min, the supernatant was discarded and cells were resuspended in fresh complete medium and then added to a new culture plate with an ultra-low attachment surface) as previously described(Gordon et al., 2019; Ye, et al., 2020).

Flow cytometric analysis of apoptosis

Adherent cells were cultured in serum-free medium to induce apoptosis and harvested 72 h after transfection. Cells were digested with 400 μl of accutase (Invitrogen), and the supernatant was collected into a 15-mL collection tube. The suspended cells and their media were also collected. The samples were centrifuged at 1000 rpm for 5 min, and the precipitate was collected and washed twice with phosphate-buffered saline (PBS). For apoptosis analysis, cells were stained using an Annexin V-FITC/propidium iodide (PI) Apoptosis Kit (MULTI SCIENCES, China). Thereafter, the cell apoptosis ratio was measured using a BD FACSVerse.

RNA fluorescence in-situ hybridization and immunofluorescence assay

Briefly, HO8910 cells were grown on a 4-chamber glass bottom dish (Cellvis, USA), fixed in a 4% formaldehyde solution and then permeabilized in PBS containing 0.5% Triton X-100. Cy3-labeled RNA fluorescence in-situ hybridization (FISH) probes targeting *RAD51B-AS1, U6* and *18S* were purchased from RiboBio Co., Ltd (China). and conducted as previously described(Guo et al., 2018). For the immunofluorescence assay, cells were blocked with 3% bovine serum albumin for 1 h. Then cells were incubated with the primary antibody anti-RAD51B (Santa cruz) at 4°C overnight and the secondary antibody FITC-labeled anti-mouse (MULTI SCIENCES) at room temperature for 1 h. After the cells were gradually washed, they were counterstained with 4′,6-diamidino-2-phenylindole (DAPI) to visualize the cell nuclei. Finally, the dish was observed under a confocal laser scanning microscope (Olympus).

Western blotting

First, the cell protein lysates were separated on a 10% sodium dodecyl sulfate-polyacrylamide gel electrophoresis gel, and then transferred to a polyvinylidene difluoride membrane. Second, western blotting analysis was performed using anti-RAD51B (Santa Cruz), anti-Bcl-2(Santa Cruz), anti-Akt (Cell Signaling Technology), anti-p-Akt (Cell Signaling Technology), and anti-β-actin (Fdbio Science) antibodies. The membrane was washed and subsequently incubated with horseradish peroxidase-conjugated secondary antibodies (Cell Signaling Technology, USA). Finally, the complexes were visualized with the Fdbio-Dura Enhanced Chemiluminescence Kit and the expression levels of proteins were assessed using ImageJ.

Mouse xenograft assay

An in vivo model of OC was established by subcutaneously injecting 3-week-old female BALB/c nude mice (Silaike Experimental Animal Co., Ltd., Shanghai, China) at a rate of 5×10^6 HO8910 cells stably overexpressing *RAD51B-AS1* (n = 12 mice), and the same number of lentivirus-infected negative control cells suspended in PBS (n = 6 mice). After 1 week, tumors were formed in both groups of nude mice, and the experimental group of LV-*RAD51B-AS1* nude mice was randomly divided into two groups: one group was injected with si-*RAD51B* intratumorally every 3 days, and the other group of nude mice and the control group of LV-NC nude mice were injected with the same amount of si-NC every 3 days to control variables. The tumor volumes of the mice were measured every week and calculated using the following formula: tumor volume [mm^3] = 0.5 × length × $width^2$). After 5 weeks, the nude mice were euthanized, and the subcutaneously implanted tumors lesions were excised, weighed, measured, and photographed. Half of the tumor tissues were used for RNA extraction, and the other half were used for immunohistochemical staining.

Immunohistochemistry analysis

Tissue samples were fixed with 4% paraformaldehyde. After adequate fixation, the tissues were pruned, dehydrated, embedded, sliced, stained, and sealed in strict accordance with the standard operating procedure for pathological experiment detection. Finally, the qualified samples were examined under a microscope. Immunohistochemical (IHC) analysis was performed using anti-RAD51B (Huabio), anti-Bcl-2(Abcam), and anti-Ki-67(Abcam) antibodies.

Statistical analysis

SPSS 24 and GraphPad Prism 8 were used for all statistical analyses. The parametric distribution of data was tested by SPSS 24.0 software. Data with Kurtosis approximately equal to zero and Shapiro-Wilk test with P value larger than 0.05 regards as Normal distribution. Student's t test was used for comparison of data showing a normal distribution and homogeneity of variance, while Welch's correction's unpaired t test was used for comparison of data showing a normal distribution but uneven variance. The nonparametric Mann–Whitney test was used for assessment of data that did not show a normal distribution. The Kaplan–Meier method was used for survival analysis. $P<0.05$ was considered a significant difference.

Table S1 Functions of lncRNAs expressed differentially between HO8910PM and HO8910

Name of lncRNAs	Expression level in HO8910PM	Function
NR_045196.2 (SNHG18)	Low	*SNHG18* acts as a tumor suppressor and a diagnostic indicator in hepatocellular carcinoma (Liu et al., 2018); promotes glioma cell motility through disruption of α-enolase nucleocytoplasmic transport (Zheng et al., 2019); indicates poor prognosis in multiple myeloma (Huang et al., 2020)(Huang, et al., 2020) and drives the growth and metastasis of non-small cell lung cancer (Fan et al., 2021)
ENST00000568391.1	High	Not reported
ENST00000607026.1	High	Not reported
NR_126480.1 (SALRNA1)	High	*SALRNA1* is a senescence-associated lncRNA that can delay senescence(Abdelmohsen et al., 2013) and is a new therapeutic target to limit the irreversible apoptosis of lung epithelial cells in patients with chronic obstructive pulmonary disease (Yuan et al., 2021).
ENST00000414885.1	High	Not reported
NR_110574.1	High	Not reported
NR_046837.1	High	Not reported
NR_125949.1	High	Not reported
NR_135108.1	High	Not reported
NR_125948.1	High	Not reported
NR_126420.1	High	Not reported
ENST00000557197.1	High	Not reported
ENST00000604215.1	High	Not reported
ENST00000599208.1	High	Not reported
ENST00000554679.1	High	Not reported
NR_027412.1 (LINC00910)	Low	*LINC00910* is hypermethylated and highly expressed in gastric cancer (Lv et al., 2020).

Table S2 LncRNAs expressed differentially between HO8910PM and HO8910

LncRNA	HO8910-1	HO8910PM-1	log_2(Fold_change)	*P*-value
NR_045196.2	0.163314	0	#NAME?	5.96E-05
ENST00000568391.1	0	0.259646	Inf	6.63E-06
ENST00000607026.1	0	0.449178	Inf	4.02E-05
NR_126480.1	0	0.168845	Inf	6.63E-06
ENST00000414885.1	0.022557	0.550219	4.608333	1.63E-07
NR_110574.1	0.020334	0.495985	4.608331	1.63E-07
NR_046837.1	0.011965	0.189694	3.986842	6.18E-05
NR_125949.1	0.005227	0.076496	3.871369	0.000142
NR_135108.1	0.025227	0.3692	3.871368	0.000142
NR_125948.1	0.005172	0.075691	3.871367	0.000142
NR_126420.1	0.033926	0.331007	3.286403	2.89E-05
ENST00000557197.1	0.077516	0.535714	2.788906	5.61E-05
ENST00000604215.1	0.098385	0.659946	2.745838	4.89E-06
ENST00000599208.1	0.163765	1.03858	2.664913	2.88E-12
ENST00000554679.1	0.142906	0.900485	2.655636	8.24E-08
NR_027412.1	0.125204	0.011746	-3.414039206	0.00011

Table S3 Prediction statistics of lncRNA target genes

Transcript	cis_num	trans_num
ENST00000554679.1	1	0

Table S4 Prediction of cis-regulation of lncRNAs

LncRNA	lnc_pos	mRNA_pos	mRNA	mRNA_symbol
ENST00000554679.1	68591721-68596913	68286496-69078703	NM_001321809.1	*RAD51B*
ENST00000554679.1	68591721-68596913	68290258-69008815	NM_001321812.1	*RAD51B*
ENST00000554679.1	68591721-68596913	68286496-68964598	NM_002877.5	*RAD51B*
ENST00000554679.1	68591721-68596913	68286496-68944810	NM_133510.3	*RAD51B*
ENST00000554679.1	68591721-68596913	68286496-69009091	NM_001321814.1	*RAD51B*
ENST00000554679.1	68591721-68596913	68286540-68944768	NM_001321817.1	*RAD51B*
ENST00000554679.1	68591721-68596913	68286496-68938393	NM_001321819.1	*RAD51B*
ENST00000554679.1	68591721-68596913	68286496-69070404	NM_001321810.1	*RAD51B*
ENST00000554679.1	68591721-68596913	68286496-69062738	NM_133509.3	*RAD51B*
ENST00000554679.1	68591721-68596913	68290309-69078678	NM_001321815.1	*RAD51B*
ENST00000554679.1	68591721-68596913	68286496-69149835	NM_001321818.1	*RAD51B*
ENST00000554679.1	68591721-68596913	68286496-69078703	NM_001321821.1	*RAD51B*

Table S5 Patient information for all specimens

Patient (ID)	Age	FIGO stage	Lymph node metastasis	CA125 (U/mL)	Diagnosis	Grade
1	73	IIB	negative	227.9	Serous Ovarian Cancer	High grade
2	46	IIIA1	positive	137.5	Serous Ovarian Cancer	High grade
3	49	IC2	negative	212.5	Serous Ovarian Cancer	High grade
4	45	IIIC	negative	894.4	Serous Ovarian Cancer	High grade
5	49	IIB	negative	215.6	Serous Ovarian Cancer	High grade
6	50	IVB	positive	258.3	Serous Ovarian Cancer	High grade
7	49	IC2	negative	22.4	Serous Ovarian Cancer	High grade
8	56	Iib	negative	174.4	Serous Ovarian Cancer	High grade
9	54	IIB	negative	1332	Serous Ovarian Cancer	High grade
10	52	IIIB	negative	272	Serous Ovarian Cancer	High grade
11	60	IIIC	positive	1401	Serous Ovarian Cancer	High grade
12	71	IIIC	positive	1475.9	Serous Ovarian Cancer	High grade
13	51	IIIC	negative	150	Serous Ovarian Cancer	High grade
14	66	IVB	negative	1216	Serous Ovarian Cancer	High grade
15	49	IIIB	positive	123	Serous Ovarian Cancer	High grade
16	61	IIIB	positive	1587	Serous Ovarian Cancer	High grade
17	57	IIIC	negative	2478	Serous Ovarian Cancer	High grade
18	66	IC2	negative	1339.7	Serous Ovarian Cancer	High grade
19	65	IIA	negative	489.5	Serous Ovarian Cancer	High grade
20	51	IIIC	positive	546.1	Serous Ovarian Cancer	High grade
21	65	IVB	negative	3118	Serous Ovarian Cancer	High grade
22	56	IIIC	positive	55.2	Serous Ovarian Cancer	High grade
23	67	IIIC	positive	1134	Serous Ovarian Cancer	High grade
24	50	IIIC	negative	8152	Serous Ovarian Cancer	High grade
25	77	IIIC	positive	3400	Serous Ovarian Cancer	High grade
26	63	IIIC	negative	8962	Serous Ovarian Cancer	High grade
27	57	IIA	negative	49	Serous Ovarian Cancer	High grade
28	51	IIIC	positive	1187	Serous Ovarian Cancer	High grade
29	45	IIIA1i	positive	1824	Serous Ovarian Cancer	High grade
30	63	IV	positive	99.8	Serous Ovarian Cancer	High grade
31	53	IIA	negative	163	Serous Ovarian Cancer	High grade
32	56	IVB	negative	70.4	Serous Ovarian Cancer	High grade
33	65	IVB	positive	610	Serous Ovarian Cancer	High grade
34	51	IIIC	negative	86	Serous Ovarian Cancer	High grade
35	77	IIIC	positive	3693	Serous Ovarian Cancer	High grade
36	74	IIIC	negative	626	Serous Ovarian Cancer	High grade
37	35	IVB	positive	1049	Serous Ovarian Cancer	High grade
38	72	IIIC	positive	551.9	Serous Ovarian Cancer	High grade
39	52	IIIC	positive	578	Serous Ovarian Cancer	High grade
40	51	IIIB	positive	849.1	Serous Ovarian Cancer	High grade
41	66	IVB	positive	4239	Serous Ovarian Cancer	High grade

42	43	IV	positive	356	Serous Ovarian Cancer	High grade
43	42	IVB	positive	571.9	Serous Ovarian Cancer	High grade
44	68	IIIC	negative	120	Serous Ovarian Cancer	High grade
45	59	IVB	positive	144	Serous Ovarian Cancer	High grade
46	53	IVB	positive	1245	Serous Ovarian Cancer	High grade
47	71	IIIA1 (ii)	positive	105.3	Serous Ovarian Cancer	High grade
48	57	IVB	positive	217.9	Serous Ovarian Cancer	High grade
49	64	IIIc	negative	82.1	Serous Ovarian Cancer	High grade
50	56			6.96	Adenomyosis	
51	74			14.5	Uterine leiomyomas	
52	54			16.5	Uterine leiomyomas	
53	49			7	Uterine leiomyomas, ovarian cysts	
54	53			5.9	Uterine leiomyomas	
55	54			11.5	Ovarian serous cystadenoma	
56	60			9.9	Ovarian cysts	
57	52			26.2	Ovarian cysts	

Table S6 Sequences of primers used for RT-qPCR in this study

Item	Sequence
β-actin	Forward: 5-ACAGAGCCTCGCCTTTGCCGAT-3’
	Reverse: 5’-CATGCCCACCATCACGCCCTG-3’
U1	Forward: 5-CCATGATCACGAAGGTGGTTT-3
	Forward: 5- ATGCAGTCGAGTTTCCCACAT-3
ENST00000568391.1	Forward: 5-CCCAAGAAGCCACCTGAAGA-3
	Forward: 5-GCATCTCCCAGGACCCTTTG-3
ENST00000607026.1	Forward: 5-CGAAAGAAACGTGGAAAGGTCG-3
	Forward: 5-GAATTCGGGCGTACTGTTTG-3
NR_126480.1	Forward: 5-ACAAGCACTCCACCAAGTCC-3
	Forward: 5-TGTTGGCCTTCACACAGCTA-3
ENST00000414885.1	Forward: 5-AGCAGATACCCTGGAAAGCC-3
	Forward: 5-AGTTTTCCTGCTTCCAGCATC-3
NR_110574.1	Forward: 5-TCGGAATGAGCACCCTTGAC-3
	Forward: 5-TGGGGTGGACCTTGTTAGGA-3
NR_046837.1	Forward: 5-GGGAAGGAATTAGGAGCGGG-3
	Forward: 5-AGTGACACAGCTCTGGTTGT-3
NR_125949.1	Forward: 5-GATGGGCGTCCACAGAATGA-3
	Forward: 5-TGATACCGTGAATGACGCCC-3
NR_135108.1	Forward: 5-AGCCTACTCATCAGGTCCACT-3
	Forward: 5-TCGTCAGCCAGAGTTCAGGA-3
NR_125948.1	Forward: 5-CCAAGGATAGCCAGTACGCC-3
	Forward: 5-ATCCTTCCGTGAATGACGCC-3
NR_126420.1	Forward: 5-AGCAAACATTACACTGGCAGC-3
	Forward: 5-CTACCAAGATGCAACTCTTGAGC-3
ENST00000557197.1	Forward: 5-TGGCCAGTGCCTGTGAGTTA-3
	Forward: 5-CAGATCGTCTGGCAGCAACAA-3
ENST00000604215.1	Forward: 5-CAATTGTTGGTGCCTCTGCAA-3
	Forward: 5-TGCAAGGATGAATACGGTAGGTC-3
ENST00000599208.1	Forward: 5-CCTTCTGCAGCTGTCGTCTA-3
	Forward: 5-GGAGGGAACCGATGCTCAAA-3
NR_045196.2	Forward: 5-GCTTCCACTCAAGTCCACCA-3
	Forward: 5-GGGTTCCAGAGAGCTCGAAG-3
NR_027412.1	Forward: 5-TCCTTGCTAACCACACGGAC-3
	Forward: 5-ATGTGGGTCCCAGTATCCGA-3
RAD51B-AS1	Forward: 5’- TCACCCCCTTAGATTCTGCATT -3’
	Reverse: 5’- TGCACTCATGCCAGCAGTAA -3’
RAD51B	Forward: 5’-CAAGAGCTGTGTGACCGTCTG-3’
	Reverse: 5’-TCATGGACACCTCGATAACTCA-3’

Table S7 Sequences of probes used for northern blotting in this study

Item	Sequence
β-actin	CTCCATCCTGGCCTCGCTGTCCACCTTCCAGCAGATGTGGATCAGCAAG CAGGAGTATGACGAGTCCGGCCCCTCCATCGTCCACCGCAAATGCTTCT AGGCGGACTATGACTTAGTTGCGTTACACCCTTTCTTGACAAAACCTAAC TTGCGCAGAAAACAAGATGAGATTGGCATGGCTTTATTTGTTTTTTTTGT TTTGTTTTGGTTTTTTTTTTTTTTTGGCTTGACTCAGGATTTAAAAACTG GAACGGTGAAGGTGACAGC
RAD51B-AS1	GAGCAGTCCCTGGCTGATACCAAGAAAACAAGACTTCAGTTCTAAAGC TGCAGAGGAATGAAATCTGCCAATAAAAGGAATGATCTTGGAAGAGGA CTATGAGCTCCAGTTTTTCTTCCAGCTCTCATGGAAACAAGCACTGCCA CAGCCCCTTGATGAGCCAGCAGAGTCCAGTCATCTGGCAACAATGACA GGTATCTGGCATCTGAGAGGAATATCAACTGAAGACAATGAGAGAATT AAAAAAGAAGTAAACACAAGACAATCTTTTTTCACCCCCTTAGATTCTG CATTTCCACTTGCTTGATTCAGTAATTGTTTTGTTTTGAATGTTGTGTAA ATGAATGCTACAGCCCTATGCAATT

Table S8 Sequences of siRNAs against specific targets in this study.

Item	Sequence
Si- *RAD51B-AS1*#1	sense: 5’- GCAUCUGAGAGGAAUAUCATT -3’
	antisense: 5’- UGAUAUUCCUCUCAGAUGCTT -3’
Si- *RAD51B-AS1*#2	sense: 5’- CCACUUGCUUGAUUCAGUATT -3’
	antisense: 5’- UACUGAAUCAAGCAAGUGGTT -3’
Si- *RAD51B*	sense: 5’- GCAAACGGCUUAUGGGAUATT -3’
	antisense: 5’- UAUCCCAUAAGCCGUUUGCTT -3’

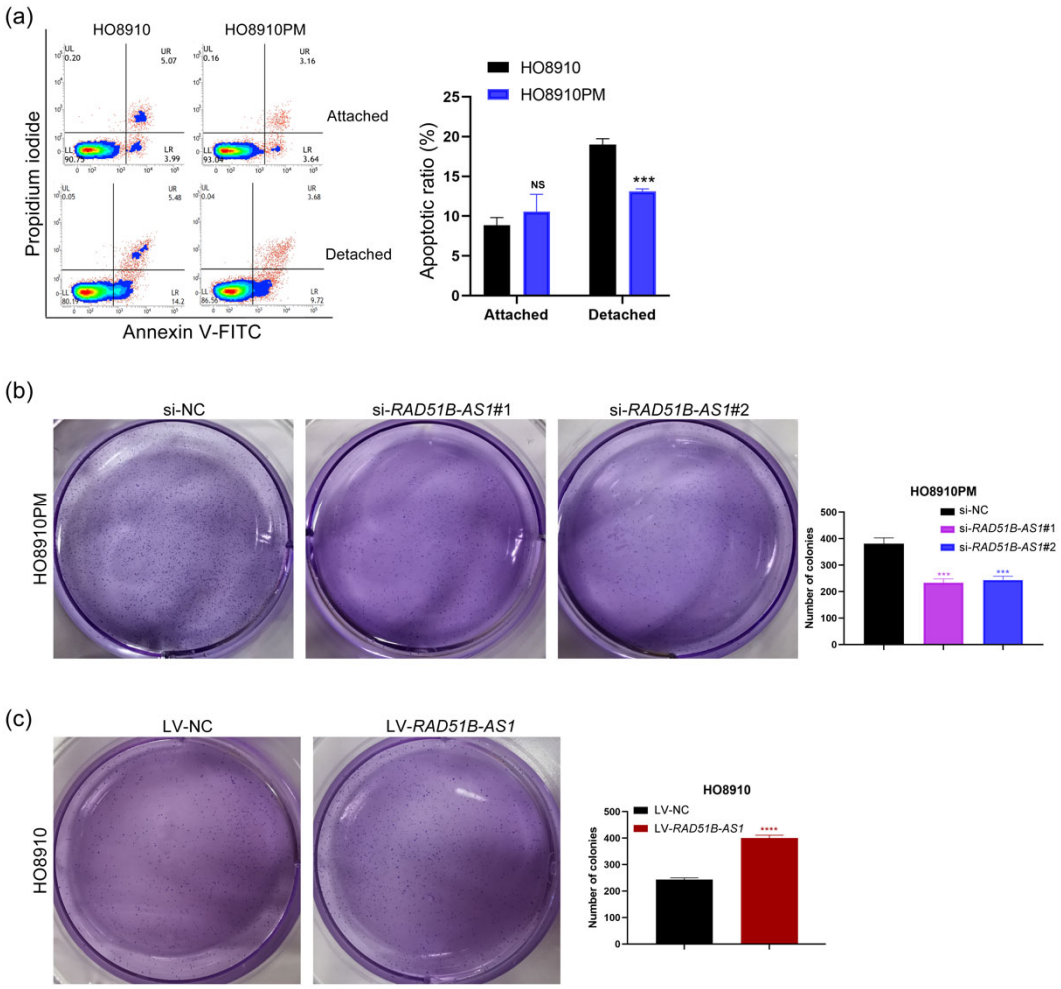

Fig. S1 Related to Figure 1. (a) Apoptosis rate of adherent and suspended cells was observed by flow cytometry. (b, c) Soft-agar assays showed anchor independent growth of HO8910PM and HO8910 cells after knocking down(b) or overexpressing(c) *RAD51B-AS1*. Results were shown as means ± SD for three separate experiments. ***p＜0.001，**p＜0.0001**

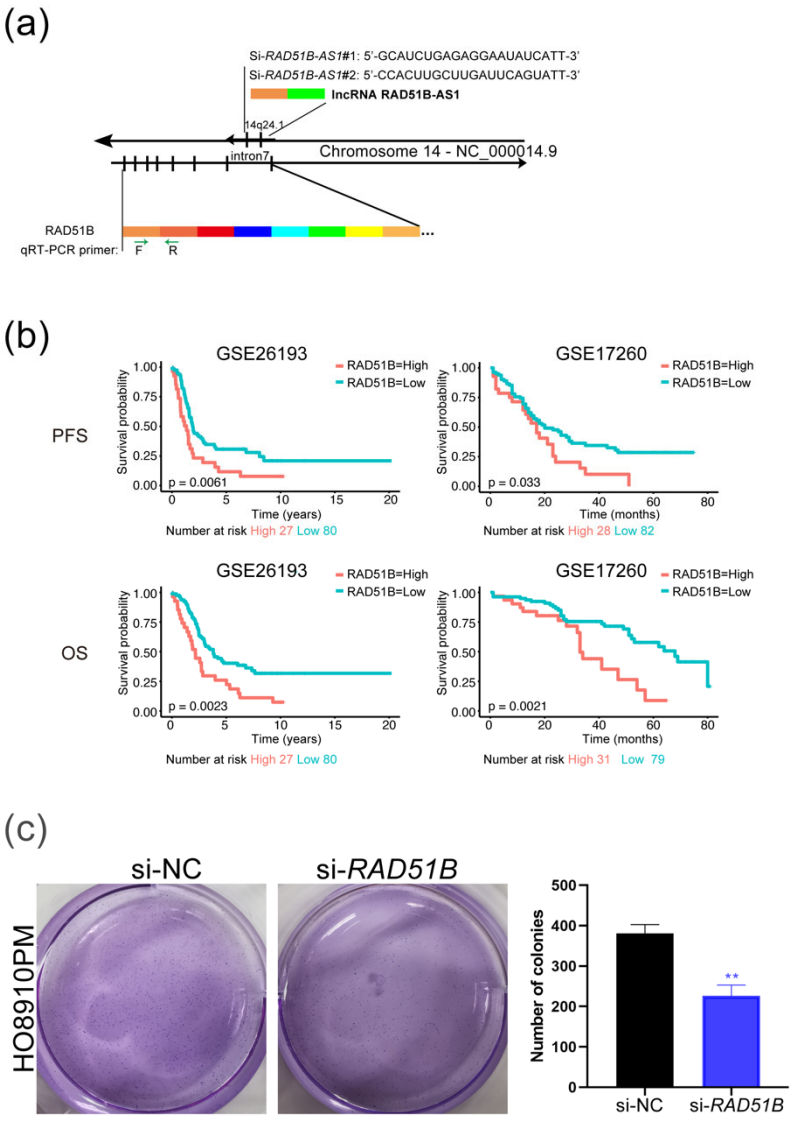

Fig. S2 Related to Figs. 3 and 4. (a) Schematic diagram of siRNAs of *RAD51B-AS1* and primers of *RAD51B*. (b) Kaplan–Meier analysis of progression-free survival and overall survival of OC patients with different RAD51B expression. (c) Soft-agar assays showed anchor independent growth of HO8910PM cells. Results were shown as means ± SD for three separate experiments. **p＜0.01

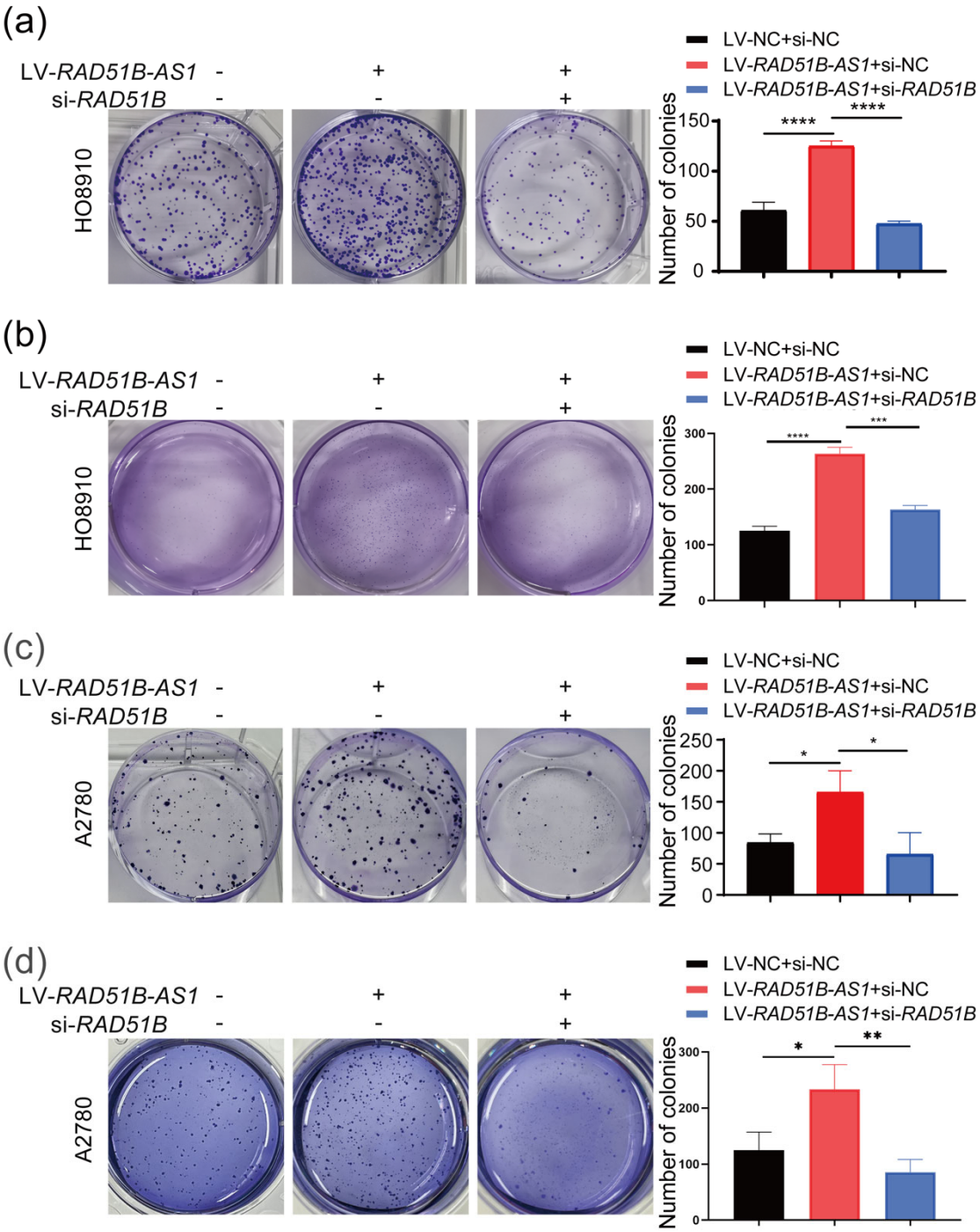

Fig. S3 Related to Fig.5. (a) The cell colony formation and viability of H08910 cells were observed by plate colony-formation experiment. (b) Soft-agar assays showed anchor independent growth of HO8910 cells. (c) The cell colony formation and viability of A2780 cells were determined by plate colony-formation assays. (d) Soft-agar assays showed anchor independent growth of A2780 cells. Results were shown as means ± SD for three separate experiments. *p＜0.05，p＜0.01，***p＜0.001，****p＜0.0001**

References

Abdelmohsen K, Panda A, Kang MJ, et al., 2013. Senescence-associated lncrnas: Senescence-associated long noncoding rnas. *Aging Cell*, 12(5):890-900. https://doi.org/10.1111/acel.12115

Fan H, Yuan J, Li Y, et al., 2021. Mkl1-induced lncrna snhg18 drives the growth and metastasis of non-small cell lung cancer via the mir-211-5p/brd4 axis. *Cell Death Dis*, 12(1):128. https://doi.org/10.1038/s41419-021-03399-z

Gordon MA, Babbs B, Cochrane DR, et al., 2019. The long non-coding rna malat1 promotes ovarian cancer progression by regulating rbfox2-mediated alternative splicing. *Mol Carcinog*, 58(2):196-205. https://doi.org/10.1002/mc.22919

Guo X, Xu Y, Wang Z, et al., 2018. A linc1405/eomes complex promotes cardiac mesoderm specification and cardiogenesis. *Cell Stem Cell*, 22(6):893-908.e896. https://doi.org/10.1016/j.stem.2018.04.013

Huang LJ, Shen Y, Bai J, et al., 2020. High expression levels of long noncoding rna small nucleolar rna host gene 18 and semaphorin 5a indicate poor prognosis in multiple myeloma. *Acta Haematol*, 143(3):279-288. https://doi.org/10.1159/000502404

Liu XF, Thin KZ, Ming XL, et al., 2018. Small nucleolar rna host gene 18 acts as a tumor suppressor and a diagnostic indicator in hepatocellular carcinoma. *Technol Cancer Res Treat*, 17:1533033818794494. https://doi.org/10.1177/1533033818794494

Lv Z, Sun L, Xu Q, et al., 2020. Joint analysis of lncrna m(6)a methylome and lncrna/mrna expression profiles in gastric cancer. *Cancer Cell Int*, 20:464. https://doi.org/10.1186/s12935-020-01554-8

Shen X, Wang C, Zhu H, et al., 2021. Exosome-mediated transfer of cd44 from high-metastatic ovarian cancer cells promotes migration and invasion of low-metastatic ovarian cancer cells. *J Ovarian Res*, 14(1):38. https://doi.org/10.1186/s13048-021-00776-2

Shen Z, Gu L, Liu Y, et al., 2022. Plaa suppresses ovarian cancer metastasis via mettl3-mediated m(6)a modification of trpc3 mrna. *Oncogene*, 41(35):4145-4158. https://doi.org/10.1038/s41388-022-02411-w

Ye G, Yang Q, Lei X, et al., 2020. Nuclear myh9-induced ctnnb1 transcription, targeted by staurosporin, promotes gastric cancer cell anoikis resistance and metastasis. *Theranostics*, 10(17):7545-7560. https://doi.org/10.7150/thno.46001

Yuan D, Liu Y, Li M, et al., 2021. Senescence associated long non-coding rna 1 regulates cigarette smoke-induced senescence of type ii alveolar epithelial cells through sirtuin-1 signaling. *J Int Med Res*, 49(2):300060520986049. https://doi.org/10.1177/0300060520986049

Zheng R, Yao Q, Li X, Xu B, 2019. Long noncoding ribonucleic acid snhg18 promotes glioma cell motility via disruption of α-enolase nucleocytoplasmic transport. *Front Genet*, 10:1140. https://doi.org/10.3389/fgene.2019.01140